Plant Molecular Biology (2020) 104:39–53
https://doi.org/10.1007/s11103-020-01022-x

GSM2, a transaldolase, contributes to reactive oxygen species homeostasis in *Arabidopsis*

Min Zheng[1,2] · Chunyan Zhu[1,2] · Tingting Yang[1,2] · Jie Qian[1,2] · Yi-Feng Hsu[1,2]

Received: 29 December 2019 / Accepted: 10 June 2020 / Published online: 20 June 2020

Abstract

Plants are exposed to various environmental cues that lead to reactive oxygen species (ROS) accumulation. ROS production and detoxification are tightly regulated to maintain balance. Although studies of glucose (Glc) are always accompanied by ROS in animals, the role of Glc in respect of ROS in plants is unclear. We isolated *gsm2* (Glc-hypersensitive mutant 2), a mutant with a notably chlorotic-cotyledon phenotype. The chloroplast-localized GSM2 was characterized as a transaldolase in the pentose phosphate pathway. With 3% Glc treatment, fewer or no thylakoids were observed in *gsm2* cotyledon chloroplasts than in wild-type cotyledon chloroplasts, suggesting that GSM2 is required for chloroplast protection under stress. *gsm2* also showed evaluated accumulation of ROS with 3% Glc treatment and was more sensitive to exogenous H_2O_2 than the wild type. Gene expression analysis of the antioxidant enzymes in *gsm2* revealed that chloroplast damage to *gsm2* cotyledons results from the accumulation of excessive ROS in response to Glc. Moreover, the addition of diphenyleneiodonium chloride or phenylalanine can rescue Glc-induced chlorosis in *gsm2* cotyledons. This work suggests that GSM2 functions to maintain ROS balance in response to Glc during early seedling growth and sheds light on the relationship between Glc, the pentose phosphate pathway and ROS.

Key message

The chloroplast-localized GSM2 is a transaldolase in the pentose phosphate pathway, which functions in the regulation of glucose-induced ROS to protect chloroplasts from oxidative damage during *Arabidopsis* early seedling growth.

Keywords GSM2 · Transaldolase · Pentose phosphate pathway · Reactive oxygen species · Glucose · Chloroplast

Introduction

Reactive oxygen species (ROS) such as the superoxide anion ($O_2^{\cdot-}$), hydrogen peroxide (H_2O_2) and the hydroxyl radical ($HO^{\cdot}$), are constantly produced during plant growth and development (Mhamdi and Van Breusegem 2018). ROS are primarily generated in chloroplasts, mitochondria and peroxisomes, but are also generated in the cell membrane, endoplasmic reticulum and nucleus (Raja et al. 2017). Due to the significant toxicity of ROS, plants have developed a set of scavenging mechanisms to remove excessive ROS and to maintain redox balance (Czarnocka and Karpinski 2018; Das and Roychoudhury 2014). When cellular antioxidant capacity cannot manage excessive ROS, oxidative stress occurs, causing damage to DNA, proteins and lipids (Demidchik 2015). Thus, ROS homeostasis plays an important role in the maintenance of normal biological processes (Foyer and Noctor 2005; Mittler 2017; Shigeoka and Maruta

Min Zheng and Chunyan Zhu have contributed equally to this work.

Electronic supplementary material The online version of this article (https://doi.org/10.1007/s11103-020-01022-x) contains supplementary material, which is available to authorized users.

✉ Yi-Feng Hsu
yifenghsu06@swu.edu.cn

[1] Key Laboratory of Eco-Environments of Three Gorges Reservoir Region, Ministry of Education, School of Life Sciences, Southwest University, Chongqing 400715, China

[2] Chongqing Key Laboratory of Plant Resource Conservation and Germplasm Innovation, Southwest University, Chongqing 400715, China

2014). For example, a physiologically permissible level of ROS is required for seed germination and dormancy (Leymarie et al. 2012). In contrast, excessive ROS impair pollen germination and tube growth (Muhlemann et al. 2018), and cause the retardation of root growth and programmed cell death (PCD) (Mira et al. 2016; Tsukagoshi 2016). It is well known that biotic and abiotic stresses can induce higher amounts of ROS, and ROS also act as signals to participate in plant stress and defense pathways and interact with phytohormones to regulate plant growth and development (Waszczak et al. 2018).

In plants, glucose (Glc) is not only an important source of energy for cellular metabolism but also a signaling molecule that regulates various developmental processes such as seed germination, seedling growth and flowering (Li and Sheen 2016). *Arabidopsis* hexokinase 1 (HXK1), the first plant Glc sensor identified, plays a dual role in Glc metabolism and signaling pathways (Moore et al. 2003). HXK1 is capable of sensing Glc and catalyzing the phosphorylation of Glc to glucose-6-phosphate (G6P), which is the initial step of glycolysis. Based on studies of Glc mutants, it has been established that an HXK1-dependent or HXK1-independent Glc/phytohormone signaling network exists (Sakr et al. 2018; Sheen 2014). While, the regulator of G protein signaling 1 (RGS1) has been also reported to regulate Glc-induced G protein signaling (Fu, et al. 2014; Janse van Rensburg, et al. 2019). In animal cells, studies of Glc metabolism and signaling are always accompanied by ROS, because high Glc from overeating carbohydrates can induce the excessive formation of ROS, which is related to some common diseases including obesity, diabetes, cancer and aging (Luo et al. 2018; Schulz et al. 2007; Semenza 2017; Shah and Brownlee 2016; Wang et al. 2014). In contrast, as an autotroph, plant produces Glc by photosynthesis for its growth and development, and the role of Glc with respect to ROS in plants is mainly focused on photosynthesis and respiration (Couee et al. 2006; Keunen et al. 2013). A recent finding revealed that autophagy-defective *Arabidopsis* mutants showed reduced Glc-induced ROS accumulation in roots (Huang et al. 2019), suggesting that ROS are important for the autophagy-mediated Glc response. Uridine 5′-diphosphoglucose (UDPG) was considered as a potential signaling molecule for the regulation of plant growth and development (Janse van Rensburg and Van den Ende 2017), and Xiao et al. (2018) found that exogenous UDPG could trigger ROS accumulation and PCD in rice (Xiao et al. 2018). However, the interaction between Glc and ROS remains to be investigated.

As an alternative metabolic pathway to glycolysis, the pentose phosphate pathway (PPP) consists of two separate phases: the oxidative and non-oxidative phases (Stincone et al. 2015). The irreversible oxidative phase produces the reducing agent NADPH, and G6P is oxidatively decarboxylated to ribulose-5-phosphate (R5P). The reversible non-oxidative phase provides glycolytic intermediates for various biosynthetic processes. Unlike the PPP in the animal cytosol, the PPP in plants is compartmentalized in the cytosol, plastids, and especially chloroplasts (Holscher et al. 2014; Kruger and von Schaewen 2003). The non-oxidative phase of the PPP in plants can also lead to the redistribution of carbon flux through the shikimate pathway for the synthesis of aromatic amino acids (AAAs) that serve as precursors for phytohormones (e.g., auxin and salicylic acid) and numerous secondary metabolites (e.g., alkaloids, flavonoids and phenylpropanoids) (Maeda and Dudareva 2012; Parthasarathy et al. 2018). In addition to transketolase, transaldolase (TA) is an important enzyme of the non-oxidative phase of the PPP that catalyzes the reaction between sedoheptulose-7-phosphate (S7P) and glyceraldehyde-3-phosphate (G3P) to yield erythrose-4-phosphate (E4P) and fructose 6-phosphate (F6P) (Caillau and Paul Quick 2005; Moehs et al. 1996). E4P and phosphoenol pyruvate (PEP) are the initial precursors of the shikimate pathway; thus, TA deficiency could affect the shikimate pathway (de Vries et al. 2018). Interestingly, some secondary metabolites from the shikimate pathway contribute to ROS scavenging (Maloney et al. 2014; Muhlemann et al. 2018; Para et al. 2016; Xu and Rothstein 2018). Although the PPP has been studied extensively in animals, its role in plant development and response to stress remains unclear.

In this study, we isolated a Glc-hypersensitive mutant, named *gsm2*, from a large-scale screen of T-DNA insertion transformants in *Arabidopsis*. *gsm2* showed chlorotic cotyledons and retarded seedling growth in the presence of 3% Glc, and the tendency for chlorosis was gradually enhanced along with an increasing concentration of Glc. GSM2 encodes a transaldolase that shares 77% sequence identity and 84% sequence similarity with tomato ToTal1. The colocalization of enhanced green fluorescent protein (EGFP) fused to GSM2 and chlorophyll reflected the chloroplast localization of GSM2. The thylakoids in *gsm2* cotyledon chloroplasts were disrupted by 3% Glc, which is consistent with the reduced chlorophyll content of *gsm2* cotyledons in response to Glc. Histochemical assays with nitro blue tetrazolium (NBT) and 3,3′-diaminobenzidine (DAB) revealed the evaluated ROS accumulation in *gsm2* cotyledons in the presence of 3% Glc. Transcriptional analysis of antioxidant enzymes further confirmed the results of NBT and DAB staining. Furthermore, the addition of diphenyleneiodonium (DPI) chloride or phenylalanine (Phe) was able to restore the greening of *gsm2* cotyledons under high Glc condition. In contrast, ethylene (ET) but not abscisic acid (ABA) could partially rescue Glc-induced cotyledon-chlorotic phenotype in *gsm2*. Taken together, these results suggest that GSM2 maintains ROS homeostasis in response to Glc during early seedling growth.

Materials and methods

Plant materials and growth conditions

Arabidopsis thaliana ecotype Columbia (Col-0) and the *gsm2-1* (SALK_202022), *gsm2-2* (SALK_206302), and *aba3-1* (CS157) mutants were obtained from the ABRC and used in this study. Seeds were surface sterilized with 10% bleach and 0.1% Triton X-100 for 7 min and washed with sterilized water three times. After stratification at 4 °C for 3 days, the sterilized seeds were plated on 1/2 Murashige and Skoog (MS) medium (PhytoTechnology Laboratories) containing various concentrations of sugar and 0.8% agar (PhytoTechnology Laboratories) at pH 5.6. To analyze the effect of H_2O_2 or ROS levels, different concentrations of H_2O_2, diphenyleneiodonium chloride, phenylalanine, and erythrose (Sigma) were added to the medium. 1–2-week-old seedlings grown on the plates were transferred to a mixture of vermiculite, perlite, and peat moss (1:1:8) and continued to grow. Plate/soil-grown plants were grown in a growth chamber under a 16-h light/8-h dark cycle at 22 °C with 8000 lx light intensity and 60% relative humidity.

Plasmid construction and plant transformation

The open reading frame of *GSM2* was cloned into the *pCAMBIA1305-HA/-EGFP* vector with the *Mlu*I and *Pst*I restriction sites, resulting in a cauliflower mosaic virus (CaMV) 35S promoter-driven construct (*35S::GSM2-HA*). The *GSM2* promoter sequence (1.5 kb region upstream of the *GSM2* start code) was cloned into the *pCAMBIA1300-GUS* vector with the *Kpn*I and *Sal*I restriction sites to generate a *GSM2p-GUS* construct. All constructs used for plant transformation were transferred to *Agrobacterium tumefaciens* GV3101 via chemical heat shock transformation. To generate stable *Arabidopsis* transgenic plants, plants were transformed by *Agrobacterium*-mediated transformation through the floral dip method (Clough and Bent 1998). The transformants were selected on 1/2 MS medium containing 20 μg/mL hygromycin (VWR). Homozygous lines from T_3 progeny were used for experiments.

RNA isolation and PCR

Total RNA was extracted using RNAiso plus (TaKaRa) according to the manufacturer's instructions. The isolated RNA from each sample was used as a template for cDNA synthesis by reverse transcription using the 5 × All-In-One RT MasterMix with an AccuRT Genomic DNA Removal kit (abm). To analyze the GSM2 transcription level in the wild type and *gsm2*, 14-day-old seedlings were used as samples for reverse transcription PCR (RT-PCR). Quantitative RT-PCR (qPCR) was performed with the LightCycler® 96 system (Roche) using EvaGreen 2 × qPCR MasterMix (abm). To analyze *GSM2* tissue-specific expression, 14-d-old seedlings and roots, 35-d-old rosette leaves/cauline leaves/stems/flower buds/siliques were used as samples. To quantify changes in *GSM2* mRNA levels in response to Glc, 9-day-old seedlings grown on sugar-free 1/2 MS medium were transferred to 1/2 MS solution containing 4.5% Glc, shaken for the indicated time points and then collected for total RNA extraction. To quantify changes in the gene expression of antioxidant enzymes or *G6PD1*, plant samples grown on 1/2 MS medium containing 1% Glc (or sugar-free 1/2 MS medium) for 6 day were collected. *ACTIN2* and *EF-1α* were used as endogenous controls (Czechowski et al. 2005). The experiments described above were independently repeated at least three times, and the data were averaged. The primers used for qPCR are listed in Supplementary Table S1.

Analysis of β-glucuronidase activity

For the histochemical visualization of β-glucuronidase (GUS) activity using the *β*-glucuronidase Reporter Gene Staining Kit (Leagene), tissues were submerged in GUS buffer supplemented with 1 × X-Gluc (5-bromo-4-chloro-3-indolyl-*β*-glucuronide) at 37 °C overnight. Then, 80% ethanol was used to wash the tissues until the chlorophyll was removed. Images were captured with a stereomicroscope (Chongqing COIC Industrial Co., Ltd., ZSA0850T, China). 9-day-old seedlings grown on sugar-free 1/2 MS medium were transferred to 1/2 MS solution containing 4.5% Glc, shaken for 6 h or 12 h and then collected.

Measurement of TA activity

TA activity assay was performed as described before (Caillau and Paul Quick 2005). Protein samples from 7-d-old seedling of the wild type, *gsm2-1* and *gsm2-2* on sugar-free 1/2 MS medium were extracted and desalted by ultrafiltration centrifugal tube (Merck Millipore Amicon Ultra, MWCO 30kD). BCA Protein Assay Kit (Novoprotein) was used to analyze protein concentration according to the manufacturer's instructions. The reaction volume of TA activity assay contained 0.4 mM of F6P (Solarbio), 0.4 mM of E4P (Sigma); 30 U triose phosphate isomerase (Shanghai yuanye Bio-Technology Co., Ltd.), 10 U D-glycerol-3-phosphate dehydrogenase (Solarbio), 0.2 mM NADH (Solarbio), and a definite volume of desalted plant extract (from 3 to 10 μL according to the samples assayed).

Enzyme activity assay

The activity of APX was tested using Ascorbate Peroxidase Assay Kit (Solarbio) according to the manufacturer's instructions. Seven-day-old wild-type, *gsm2-1* and *gsm2-2* grown on 1/2 MS medium containing 3% Glc (or sugar-free 1/2 MS medium) were used as samples.

Chlorophyll measurement and fluorescence

Seven-day-old wild-type, *gsm2-1* and *gsm2-1* complement line 1 seedlings grown on 1/2 MS medium containing 3% Glc (or sugar-free 1/2 MS medium) were used as samples. Chlorophyll was extracted from the plant samples with 80% acetone, and the chlorophyll content was measured using a spectrophotometer (Pultton, P100+, USA) at 645 nm and 663 nm according to previous methods (Porra 2002). Imaging of the chlorophyll signal in the cotyledons of plant samples was performed by measuring chlorophyll autofluorescence following excitation with a 488 nm argon laser and detection at 650 nm (Olympus FV1000).

Chloroplast ultrastructure analysis

Fully expanded cotyledons from 7-day-old wild-type, *gsm2-1* and *gsm2-1* complement line 1 seedlings grown on 1/2 MS medium containing 3% Glc (or sugar-free 1/2 MS medium) were used for transmission electron micrography. Plants were fixed overnight at room temperature by vacuum infiltration with a 2.5% (w/v) glutaraldehyde solution (Sigma), washed three times with phosphate buffer (Biosharp), postfixed with 1% (w/v) osmium tetroxide (Sigma) for 3 h and washed again in a similar manner. After fixation, the samples were dehydrated with a graded ethanol series and embedded in Spurr resin (SPI-812) with a propylene oxide (Chuandong Chemical) mixture. The resin was polymerized at 60 °C for 48 h. Ultrathin sections were cut on a Leica EM UC7 ultramicrotome (Leica Microsystems) and stained with 3% (w/v) lead citrate (Sigma) and 2% (w/v) uranyl acetate (Daken Chemical) before being observed with a transmission electron microscope (JEOL JEM-1400 Plus electron microscope).

Histochemical staining of dead cells and ROS

Wild-type and *gsm2* seedlings were grown on 1/2 MS medium containing 3% Glc (or sugar-free 1/2 MS medium). Dead cells were assessed by Trypan blue staining as described previously (Tanaka et al. 2004). Plants were incubated with a 1% (w/v) Trypan blue (Sigma) solution at room temperature overnight and then washed with phosphate buffer (Biosharp). For the detection of $O_2^{\cdot-}$or H_2O_2, plants were stained overnight with 0.1% (w/v) NBT (neoFroxx) or DAB (Sigma) and then bleached by boiling in an ethanol:glycerol:acetic acid (3:1:1) solution for 10 min. Images were captured with a stereomicroscope (Chongqing COIC Industrial Co., Ltd., ZSA0850T, China).

Confocal microscopy analysis and imaging

Mesophyll protoplasts were prepared as previously described (Yoo et al. 2007). Transformed *Arabidopsis* mesophyll protoplasts were observed after transformation 48 h with a laser scanning confocal microscope (Nikon C2-ER). Fluorescent signals were detected using an argon laser with a 488 nm excitation wavelength and a 510 nm bandpass filter to detect EGFP and a 650 nm bandpass filter to detect chlorophyll.

Statistical analysis

All the experiments were performed with at least three technical replicates on two to four biological replicates. Data were analyzed with GraphPad Prism 5 and Microsoft Excel 2010 (Microsoft) for calculating mean and standard error (SE), except qPCR which was used LightCycle® 96 SW1.1 software. The statistical significance was determined using the standard Student's *t* test.

Accession numbers

Sequence data from this article can be found in the TAIR (The Arabidopsis Information Resource) or GenBank database under the following accession numbers: *GSM2* (*AT5G13420*), *GSM2-LIKE* (*AT1G12230*), *ABA3* (*AT1G16540*), *CAT1* (*AT1G20630*), *CAT2* (*AT4G35090*), *CSD1* (*AT1G08830*), *CSD2* (*AT2G28190*), *sAPX* (*AT4G08390*), *tAPX* (*AT1G77490*), *2CPA* (*AT3G11630*), *2CPB* (*AT5G06290*), *EF-1α* (*AT1G18070*), *ACTIN2* (*AT3G18780*), *G6PD1* (*AT5G35790*), *ToTal1* (*AF184164*), *ToTal2* (*AY007225*).

Results

The loss of GSM2 function leads to cotyledon chlorosis in response to Glc

As in our previous studies, a genetic screen to identify Glc-hypersensitive or Glc-insensitive mutants was carried out in *Arabidopsis* (Hsiao et al. 2016; Hsu et al. 2014; Zheng et al. 2019). Thousands of T-DNA insertion mutants were grown on 1/2 MS medium containing 3% Glc or mannitol as a control. After 14 d, *gsm2-1* (glucose hypersensitive mutant 2) showed obvious chlorotic cotyledons as well as retarded seedling growth (Fig. 1a). The true leaves in *gsm2-1* displayed a normal green color similar to that in the wild type.

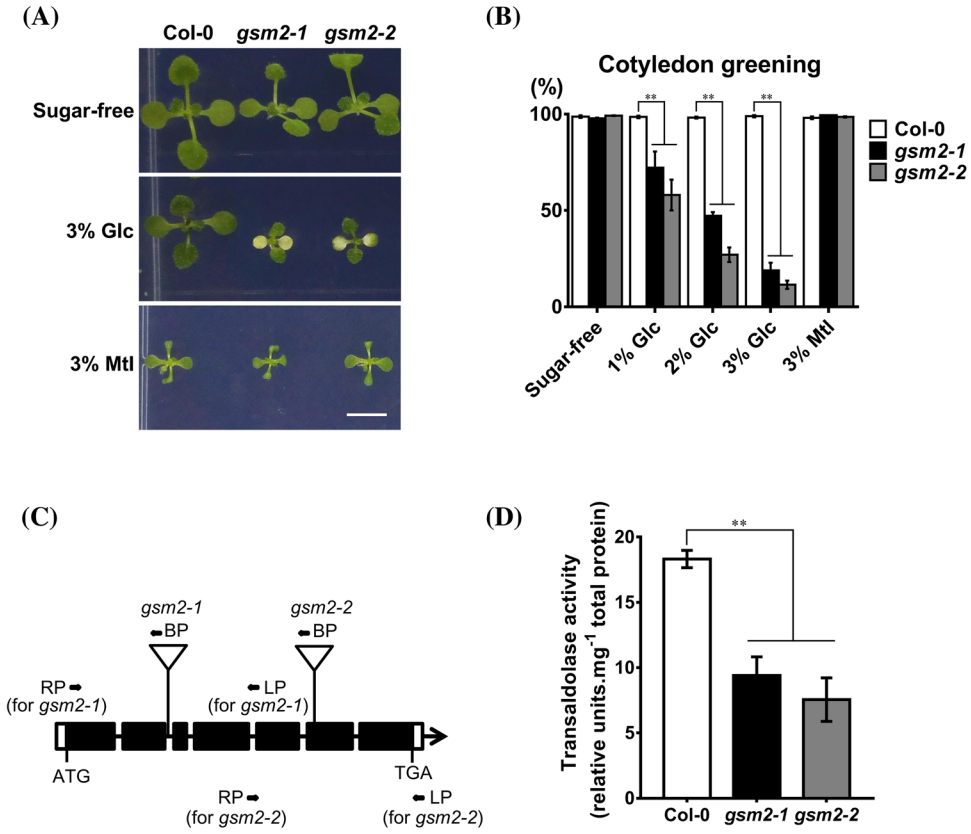

Fig. 1 Isolation of *Arabidopsis* T-DNA insertion mutants with hypersensitivity to Glc. **a** The Glc-hypersensitive phenotype of *gsm2*. **b** Statistical analysis of the cotyledon greening rate of 9-day-old Col-0 (the wild type), *gsm2-1* and *gsm2-2* grown on 1/2 MS medium supplemented with increasing amounts of Glc (sugar-free, 1%, 2%, 3%) or Mtl as a control. **c** Schematic diagram of *GSM2* and T-DNA insertion sites in *gsm2-1* and *gsm2-2*. Black boxes, exons; lines, introns; white boxes, the untranslated regions; inverted triangles, T-DNA insertion sites. Arrows indicate primers used for genotyping (LP/RP, left/right genomic primers; BP, T-DNA border primer). **d** Analysis of TA activity in Col-0, *gsm2-1* and gsm2-2 on sugar-free 1/2 MS medium. Error bars represent the standard deviation (SD; *t* test: $^{**}P < 0.01$). Scale bar, 5 mm

Treatment with 3% mannitol did not affect cotyledon greening in *gsm2-1*. Cotyledon chlorosis in *gsm2-1* was gradually enhanced with increasing Glc concentration. Compared to that of completely green cotyledons in wild-type plants, the greening rate of *gsm2-1* cotyledons was 72.1% in 1% Glc, 47.2% in 2% Glc and 18.9% in 3% Glc (Fig. 1b), suggesting that the chlorotic-cotyledon phenotype is correlated with Glc and not due to osmotic stress. Chlorosis was also observed in *gsm2-1* cotyledons treated with 3% sucrose (Suc), but this effect was not as severe as that following treatment with Glc (Supplementary Fig. S1a). To further characterize the hypersensitivity of *gsm2-1* to Glc, the germination rate was determined (Supplementary Fig. S1b). A significant difference in germination rate was found after 2 d of 3% Glc treatment, where more than 70% of wild-type plants germinated, whereas the germination rate of *gsm2-1* was approximately 20%. After 4 d, *gsm2-1* and the wild type exhibited a similar germination rate, which was nearly 100%. Upon treatment with 4.5% Glc, *gsm2-1* germinated at a lower rate than the wild type.

The T-DNA insertion site in *gsm2-1* was determined to be in the intron of *AT5G13420* (Fig. 1c), which was thought to encode a transaldolase. From an amino acid sequence similarity-based BLAST search, GSM2 shows high sequence similarity to ToTal1 in tomato, with 77% and 84% sequence identity and similarity, respectively (Supplementary Fig. S2a). Caillau and Paul Quick (2005) reported that ToTal1, in contrast to its isoform ToTal2, showed TA catalytic activity and was involved in plant pathogen infection (Caillau and Paul Quick 2005). In *Arabidopsis*, although the GSM2-like protein (GSL) shares only 21% and 32% sequence identity and similarity, respectively, with GSM2 (Supplementary Fig. S2b), it shares 65% and 78% sequence identity and similarity, respectively, with ToTal2 (Supplementary Fig. S3). It has been noted that TA in plants contains a well conserved amino acid sequence required for its enzyme activity in the non-oxidative phase of the PPP (Supplementary Fig. S4). To further explore the role of GSM2 in early seedling growth, we obtained another *gsm2* mutant allele (*gsm2-2*) from the Arabidopsis Biological Resource Center (ABRC), in which the T-DNA is inserted in the sixth exon of *AT5G13420* (Fig. 1c). Genomic PCR and RT-PCR analysis revealed that the *AT5G13420* transcript was not detected in homozygous mutants (Supplementary Fig. S5a), suggesting that both *gsm2-1* and *gsm2-2* are transcriptional knockouts. We examined the transaldolase activity of *gsm2*. Both of *gsm2-1* and *gsm2-2* showed about twofold lower transaldolase activity than that in the wild type (9.4 in *gsm2-1*, 7.6 in *gsm2-2* and 18.3 in the wild type) (Fig. 1d). Similar to *gsm2-1*, *gsm2-2* also exhibited cotyledon chlorosis in 3% Glc (Fig. 1a, b). The transgenic overexpression of full-length *AT5G13420* cDNA in *gsm2-1* was able to complement Glc-induced

cotyledon chlorosis and the growth arrest of *gsm2-1* (Supplementary Fig. S5b). Taken together, these results suggest that the disruption of *AT5G13420* results in the hypersensitivity of *gsm2* to Glc.

GSM2 is localized to the chloroplast

To investigate the tissue-specific expression of *GSM2*, we cloned a 1.5 kb region upstream of the *GSM2* start codon that acts as its native promoter to drive the reporter gene GUS. The *GSM2p-GUS* transcriptional fusion construct was introduced into *Arabidopsis* to generate stable transgenic lines. GUS activity was detectable in all tested tissues including roots, rosette leaves, cauline leaves, stems, flower buds, siliques and seedlings (Fig. 2a). The results from qPCR analysis of the *GSM2* transcript in wild-type plants showed that seedlings, rosette leaves and roots had higher expression level of *GSM2* than other tested tissues (Fig. 2b). qPCR was used to examine the expression level of *GSM2* in 3- to 7-day-old seedlings (Fig. 2c). *GSM2* expression did not differ markedly across 3- to 6-d-old seedlings but was rapidly promoted in 7-d-old seedlings; *GSM2* expression in 7-day-old seedlings was over twofold higher than that in 3- to 6-d-old seedlings. Since *gsm2* is hypersensitive to Glc, the effect of Glc on the expression of *GSM2* was evaluated. *GSM2* expression was increased with prolonged treatment with Glc, and GUS activity was also induced by Glc (Fig. 2d, e).

Consistent with the Glc-induced yellow or pale color of *gsm2-1* cotyledons, the level of chlorophyll content was severely reduced in *gsm2-1* with 3% Glc treatment compared to that in the wild type (Fig. 3a), which was also corroborated by the examination of chlorophyll autofluorescence (Fig. 3b). Next, we analyzed the ultrastructure of chloroplasts in *gsm2-1* cotyledons by transmission electron microscopy (Fig. 3c). Compared to the wild-type chloroplasts, the

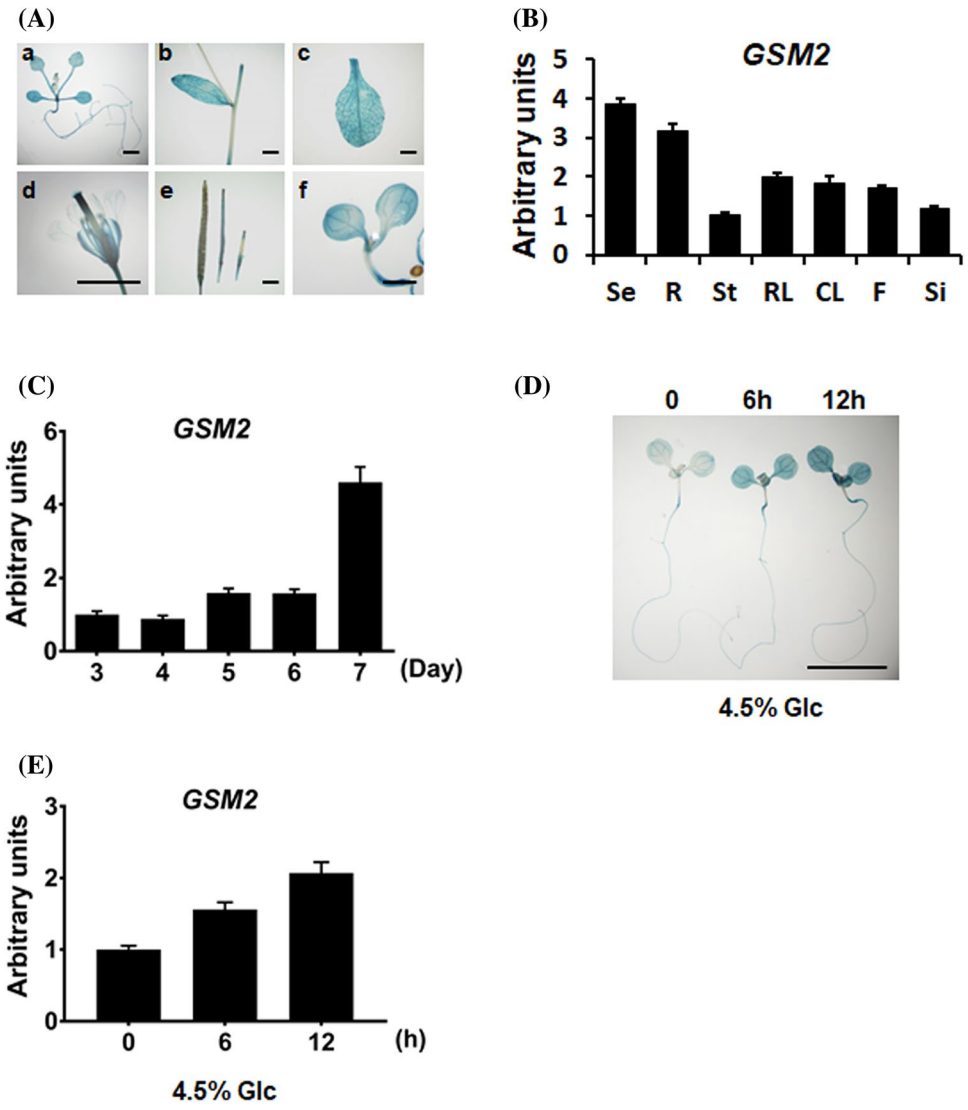

Fig. 2 Expression analysis of *GSM2*. **a** Tissue-specific expression of *GSM2p-GUS* in Col-0. Representative images: a. 14-day-old seedlings/roots; **b**–**e**. 35-day-old cauline leaves/stems, rosette leaves, flower buds, and siliques; and **f** 7-day-old seedlings. **b** qPCR analysis of *GSM2* expression in Col-0 (*Si* siliques, *F* flower buds, *St* stems, *CL* cauline leaves, *RL* rosette leaves, *R* roots, *Se* seedlings). qPCR analysis of *GSM2* expression **c** during early seedling growth (3 to 7 day) or **e** in response to 4.5% Glc (0 to 12 h). **d** *GSM2p-GUS* staining pattern in 9-d-old Col-0 seedlings upon treatment with 4.5% Glc. *EF-1α* (**b**) and *ACTIN2* (**c**, **e**) were used as endogenous controls. Error bars represent the standard deviation (SD). Scale bar: **a** 1 mm; **d** 5 mm

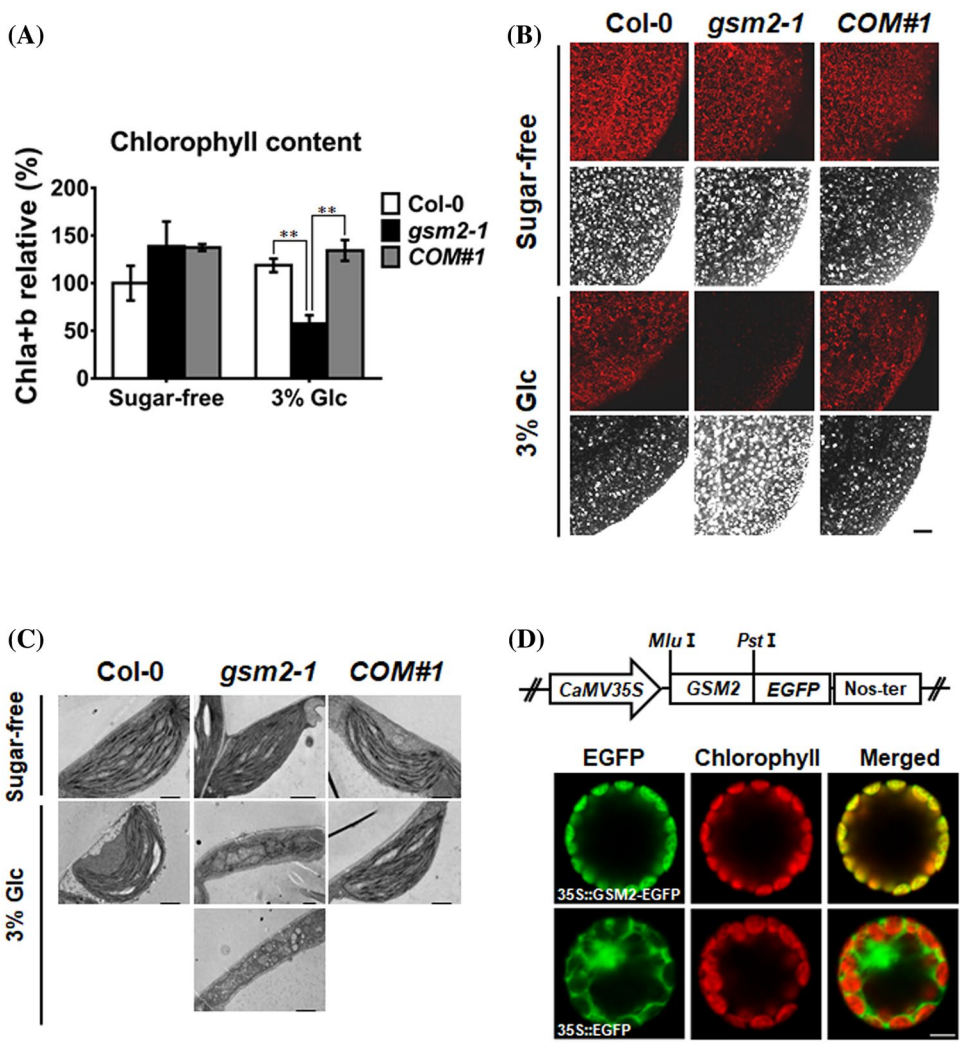

Fig. 3 The loss of GSM2 affects the development of cotyledon chloroplasts in the presence of Glc. **a** The chlorophyll content of *gsm2-1* was reduced in response to 3% Glc. **b**, **c** Analysis of chlorophyll autofluorescence and chloroplast ultrastructure in Col-0, *gsm2-1* and *COM#1* cotyledons grown on 1/2 MS medium containing 3% Glc (or sugar-free 1/2 MS medium). **d** GSM2 is localized to the chloroplasts. Top: diagrammatic representation of the *35S::GSM2-EGFP* construct used to test GSM2 localization. Bottom: subcellular localization of the GSM2-EGFP fusion protein in mesophyll protoplasts. EGFP signals are shown in green. Chlorophyll autofluorescence signals are shown in red. The colocalization between GSM2-EGFP and chlorophyll is indicated by yellow. Error bars represent the standard deviation (SD; *t* test: *ns* no significant difference, $^{**}P < 0.01$). Scale bar: **b** 100 μm; **c** 1 μm; **d** 10 μm

gsm2-1 chloroplasts appeared misshapen with few or no thylakoid membrane systems in 3% Glc, and the chloroplast defects were fully rescued in the *gsm2-1* complement line 1. These results suggest that the *gsm2* chloroplasts could respond to Glc. To further investigate the effect of Glc on chloroplast development in *gsm2* cotyledons, *gsm2* and the wild type were grown on 1/2 MS medium containing 3% Glc for 5 d and then transformed to 1/2 MS medium supplemented with 0%, 3% or 4.5% Glc for 9 d. In addition to retarded growth, chlorotic *gsm2* cotyledons were still observed (Supplementary Fig. S6 right panel). Nevertheless, when *gsm2* and the wild type were grown on sugar-free 1/2 MS medium (instead of 3% Glc-containing 1/2 MS medium) for 5 d before transfer, *gsm2* showed normal growth and green cotyledons that were similar to those seen in the wild type (Supplementary Fig. S6 left panel). These results elucidate that GSM2 plays an important role in the early stage of cotyledon chloroplast development. In addition, TA is restricted to plastids in plants (Caillau and Paul Quick 2005); therefore, we speculated that chloroplasts might be targeted by GSM2. To assess GSM2 subcellular localization, GSM2 was fused to the N-terminus of EGFP driven by a CaMV 35S promoter. GSM2-EGFP was transiently expressed in *Arabidopsis* leaf protoplasts. As expected, the green fluorescence of GSM2-EGFP exclusively localized with the chlorophyll autofluorescence (Fig. 3d), revealing the chloroplast localization of GSM2.

Glc-induced ROS accumulation in *gsm2*

Considering the chlorophyll deficiency and aberrant chloroplasts observed in *gsm2* cotyledons in 3% Glc, both the photosynthetic capacity and productivity of *gsm2* were thought to be decreased, which might induce carbon starvation and ultimately cell death. Therefore, we used Trypan blue staining to monitor cell death. Dark blue stain was clearly observed in *gsm2* cotyledons with 3% Glc treatment compared to that in wild-type cotyledons (Fig. 4a right panel), whereas the stain was not found in either the untreated wild-type or *gsm2* cotyledons (Fig. 4a left panel), implying that

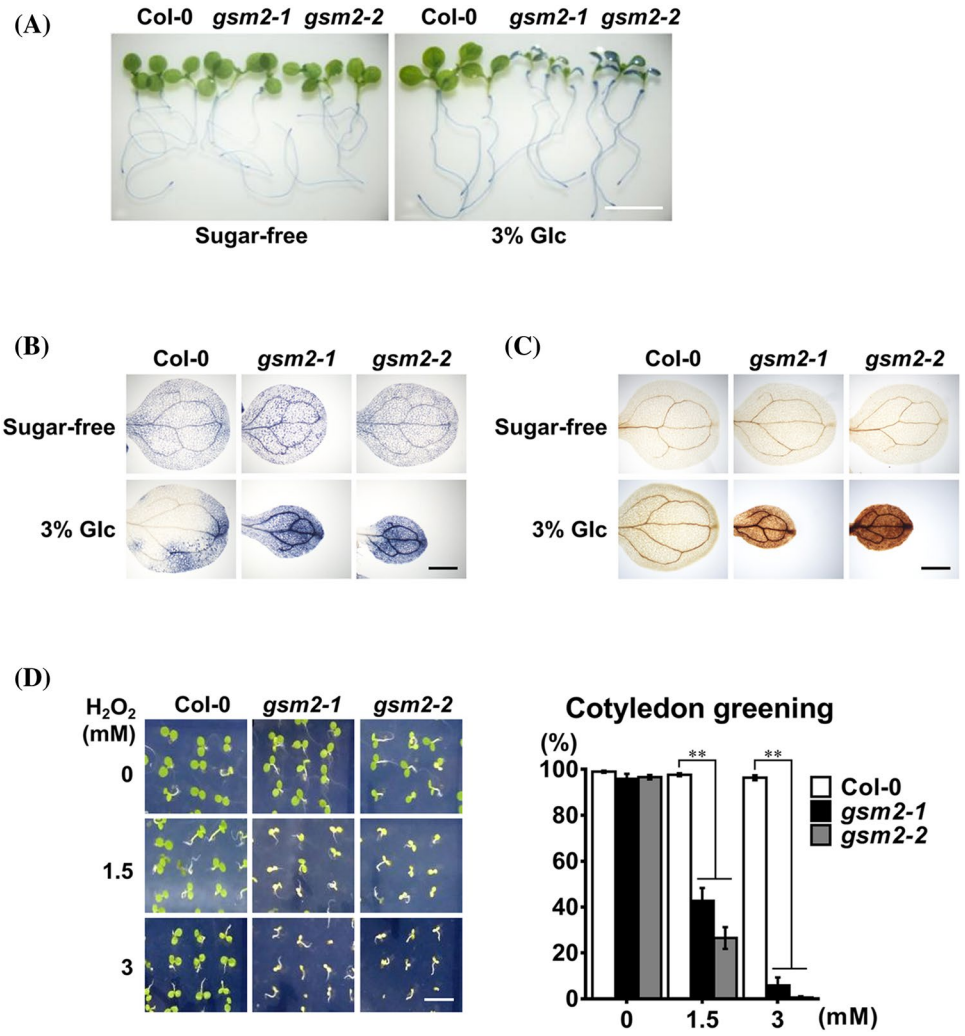

Fig. 4 Cell death and ROS accumulation in *gsm2* cotyledons in response to Glc. **a**–**c** Staining with **a** Trypan blue to measure cell death, **b** NBT to measure $O_2^{\cdot-}$, and **c** DAB to measure H_2O_2 in Col-0, *gsm2-1* and *gsm2-2* grown on 1/2 MS medium containing 3% Glc (or sugar-free 1/2 MS medium). **d** Effects of H_2O_2 on Col-0, *gsm2-1* and *gsm2-2*. Left: representative images. Right: statistical analysis of the cotyledon greening rate. Error bars represent the standard deviation (SD; *t* test: $^{**}P < 0.01$). Scale bar: **a**, **d** 5 mm; **b**, **c** 0.5 mm

cell death occurred in the 3% Glc-treated *gsm2* cotyledons. It is well known that cell death is accompanied by excessive accumulation of ROS. To evaluate ROS accumulation in *gsm2*, staining with NBT or DAB was used to examine the production of $O_2^{\cdot-}$ and H_2O_2, respectively. NBT is reduced by $O_2^{\cdot-}$ to blue formazan, and DAB reacts with H_2O_2 to exhibit a brown precipitate (Kumari et al. 2015). Untreated wild-type and *gsm2* seedlings showed similar basal $O_2^{\cdot-}$ and H_2O_2 levels (Fig. 4b, c upper panel). The accumulation of $O_2^{\cdot-}$ or H_2O_2 in *gsm2* cotyledons was notably enhanced upon treatment with 3% Glc, which produced dark blue and brown staining (Fig. 4b, c lower panel; Supplementary Fig. S7). In contrast, NBT staining in the 3% Glc-treated wild-type cotyledons appeared slightly less intense (or even pale) than that in the untreated cotyledons (Fig. 4b lower panel). In accordance with the higher endogenous level of ROS in *gsm2*, 1.5 mM H_2O_2 was sufficient to induce chlorosis in *gsm2* cotyledons, which also inhibited the root growth in both the wild type and *gsm2* (Fig. 4d). Whereas, at least 50% of *gsm2* was not able to grow the true leaf because of the strong inhibitory effect of H_2O_2 on *gsm2* (Supplementary Fig. S8). On the other hand, we found that 3% Glc did not induce cell death in *gsm2* grown in the dark and that both *gsm2* and wild-type cotyledons were still etiolated with Trypan blue treatment (Supplementary Fig. S9 left panel). After *gsm2* grown in the dark was transferred to light for an additional 3 day, a sharp increase in the permeability to Trypan blue was detected in *gsm2* cotyledons (Supplementary Fig. S9 right panel), which suggested that Glc might have an additive effect on light-induced ROS production and enhance the severity of oxidative damage, ultimately resulting in cell death. These results indicated that Glc-induced ROS accumulation is associated with cell death in *gsm2* cotyledons.

Gene expression of antioxidant enzymes in *gsm2*

As we observed, *gsm2* displayed chlorotic cotyledons and the excessive accumulation of ROS in the presence of Glc, which raised the question of whether the impairment of redox balance is responsible for chlorosis. Thus, we

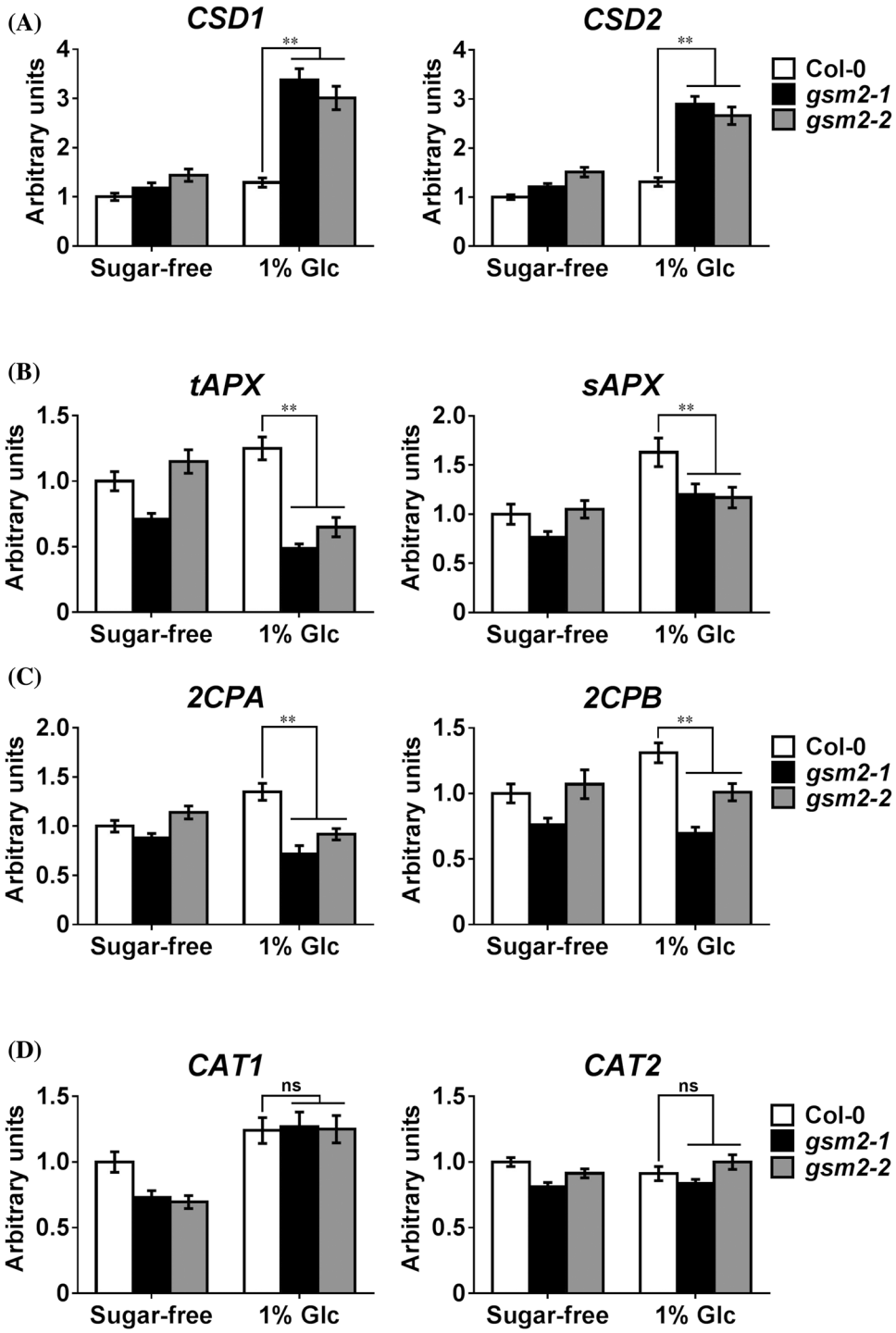

Fig. 5 The gene expression of the antioxidant enzymes. **a** *CSD1* and *CSD2*; **b** *tAPX*, *sAPX*, *2CPA* and *2CPB*; and **c** *CAT1* and *CAT2* in response to Glc during early seedling growth. Total RNA was extracted from 6-day-old seedlings grown on 1/2 MS medium containing 1% Glc (or sugar-free 1/2 MS medium). *ACTIN2* was used as an endogenous control. Error bars represent the standard deviation (SD; *t* test: ns, no significant difference, $^{**}P < 0.01$)

examined the gene expression of ROS scavenging enzymes. With 1% Glc treatment, the transcript levels of *CSD1* (CuZn-superoxide dismutase 1) and *CSD2* (CuZn-superoxide dismutase 2) in *gsm2* were by 3 to 4-fold higher than those in the wild type (Fig. 5a). The most prominent chloroplast peroxidases were sAPX (stromal ascorbate peroxidase), tAPX (thylakoid-bound ascorbate peroxidase), 2CPA (2-Cys peroxiredoxin A) and 2CPB (2-Cys peroxiredoxin B). Upon 1% Glc treatment, the expression levels of the four genes in *gsm2* were significantly decreased compared to those in the wild type (approximately one-fold decrease in *tAPX*, *2CPA* or *2CPB*) (Fig. 5b). We tested APX activity in *gsm2* and the wild type. With or without Glc treatment, the activity of APX in *gsm2* was obviously lower than that in the wild type (Supplementary Fig. S10). While *CAT1* (catalase 1) and *CAT2* (catalase 2) transcript levels remained similar in

gsm2 and the wild type with and without 1% Glc treatment (Fig. 5c). Superoxide dismutase is capable of dismutating $O_2^{\cdot-}$ into H_2O_2, and peroxidases and catalases detoxify H_2O_2 to maintain ROS homeostasis. In response to Glc, *CSD1*/*CSD2* expression in *gsm2* was strongly induced to cope with the massive production of $O_2^{\cdot-}$; however, *tAPX*/*2CPA*/*2CPB* expression was downregulated, and did not increase along with *CSD1*/*CSD2* expression and could not efficiently reduce the enhanced levels of H_2O_2 to water, which probably resulted in oxidative damage to the chloroplasts in *gsm2* cotyledons.

DPI and Phe rescue Glc-induced chlorosis in *gsm2* cotyledons

Considering the putative function of GSM2 in the PPP, we examined the effects of different additives related to the PPP on Glc-induced chlorosis in *gsm2* cotyledons. 1 μM DPI, an NADPH oxidase inhibitor (Kleniewska et al. 2012), was added to 1/2 MS medium containing 3% Glc (or sugar-free 1/2 MS medium). With application of DPI in sugar-free 1/2 MS medium, *gsm2* was not markedly different from the wild type (Fig. 6a). In contrast, with application of DPI in 3% Glc-containing 1/2 MS medium, the Glc-induced chlorotic phenotype of *gsm2* cotyledons was complemented (Fig. 6b) and the Glc-induced extensive staining of *gsm2* cotyledons by DAB was also alleviated, suggesting that H_2O_2 was highly reduced (Supplementary Fig. S11). We also found that upon treatment of 1% Glc, the transcript level of glucose-6-phosphate dehydrogenase 1 (*G6PD1*) in *gsm2* was significantly almost onefold lower than that in the wild type (Fig. 6b). Previous studies have demonstrated the important role of Phe in *Arabidopsis* etiolated seedlings (Para et al. 2016). Accordingly, we evaluated the effect of Phe on Glc-induced chlorosis in *gsm2* cotyledons. The addition of 500 μM Phe to 3% Glc successfully rescued Glc-induced chlorosis in *gsm2* cotyledons (Fig. 6c). Whereas, erythrose (Ery) had no effect on the greening of chlorotic *gsm2* cotyledons in 3% Glc (Fig. 6c).

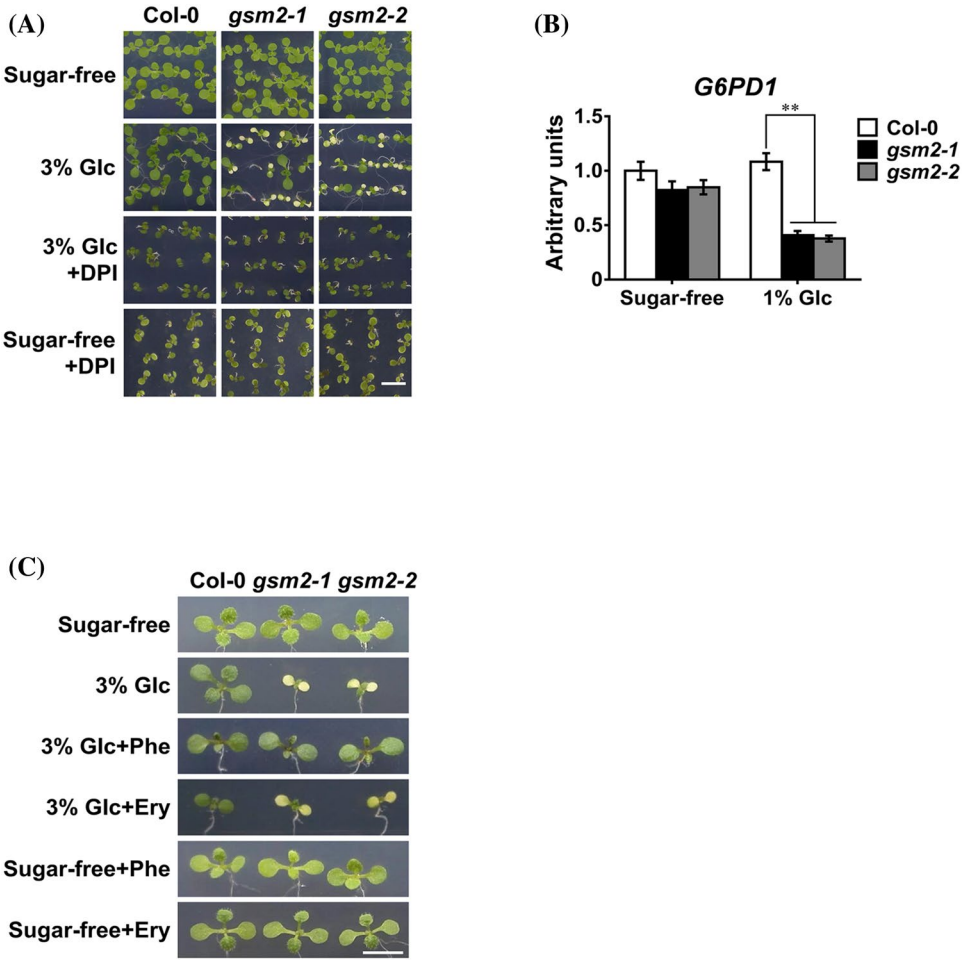

Fig. 6 Effects of additives on Glc-induced cotyledon chlorosis in *gsm2*. **a** The addition of DPI can restore Glc-induced cotyledon chlorosis in *gsm2*. **b** The Glc-induced decrease of *G6PD1* transcripts in *gsm2*. **c** Effects of Phe and Ery on Glc-induced cotyledon chlorosis in *gsm2*. Error bars represent the standard deviation (SD; *t* test: *ns* no significant difference, $^{**}P < 0.01$). Scale bar, 5 mm

The effect of ABA or ET on Glc-induced chlorosis in *gsm2* cotyledons

Previous studies have demonstrated that ABA and ET have antagonistic effects on the plant response to Glc (León 2003). Accordingly, we evaluated the effect of ABA and ET on *gsm2*. With treatment of 0.1 µM or 0.2 µM ABA, *gsm2* was more sensitive to ABA than the wild type, which still showed normal green cotyledons (Supplementary Fig. S12). *gsm2-1* was crossed with *aba3-1*, an ABA-deficient mutant, to generate a *gsm2-1 aba3-1* double mutant. Similar to *gsm2-1*, *gsm2-1 aba3-1* had chlorotic cotyledons when treated with 3% Glc (Supplementary Fig. S13a), which indicated that the chlorotic phenotype of *gsm2* cotyledons involves ABA-independent Glc signaling. In contrast, although *gsm2* and the wide type appeared similar in 10 µM 1-aminocyclopropane-1-carboxylic acid (ACC) used to produce ET and displayed normal green cotyledons (Supplementary Fig. S13b upper panels), the addition of 10 µM ACC in the presence of 3% Glc reduced the Glc-hypersensitivity of *gsm2* and partially restored greening in *gsm2* cotyledons (Supplementary Fig. S13b lower panels).

Discussion

The role of GSM2 in the PPP

A BLAST search revealed that many monocotyledonous and dicotyledonous plants have GSM2 homologs (Supplementary Fig. S4). GSM2 is thought to encode a PPP enzyme, TA, which is responsible for catalyzing the reaction between S7P and G3P to yield E4P and F6P in the non-oxidative phase of the PPP. The non-oxidative phase of the PPP not only acts as a source of NADPH as well as the oxidative phase, but also provides intermediates for various biosynthetic processes. TA, in conjunction with TK, plays an important role in converting R5P to G6P during the non-oxidative phase of the PPP. However, in animals, TA is not expressed in certain organisms and tissues (Perl et al. 2006), and the non-oxidative phase could function without this enzyme (Qian et al. 2008). Hence, it has not been established that TA acts as a regulator through the PPP in the modulation of distinct physiological and metabolic processes. TA deficiency impairs mitochondrial function to cause mice infertility and increases the *Caenorhabditis elegans* lifespan (Bennett et al. 2017; Perl et al. 2006). In humans, TA is implicated in liver diseases and cancer cell proliferation (Perl et al. 2011). The function of TA in plants is still poorly understood, although it has been a few decades since TA was initially discovered in peas. TA abundance in both wheat and cucumber leaves was largely promoted with fungal infection (Caillau and Paul Quick 2005). Yang et al. (2015) recently reported that rice TA knockout plants showed a dwarfed phenotype with shorter and narrower leaves, altered culm elongation and vascular pattern (Yang et al. 2015). *tra2*, another *gsm2* knockout mutant, exhibited the low-lignin trait and increased saccharification efficiency, which suggested its role in leading carbohydrate flux toward phenolic metabolism (de Vries et al. 2018; Vanholme et al. 2012).

Based on this study, we suspect that the PPP is related to the elevated ROS in *gsm2* in response to Glc. First, lower GSM2 levels may indirectly affect the amount of NADPH, which is required to minimize oxidative damage from ROS and maintain redox homeostasis. As an NADPH oxidase inhibitor, DPI was used to assess the requirement of NADPH for removing ROS by adding 1 µM DPI to 3% Glc-containing 1/2 MS medium, which restored *gsm2* cotyledon greening (Fig. 6a). Glucose-6-phosphate dehydrogenase (G6PDH) catalyzes the oxidation of G6P to 6-phosphogluconolactone and generates NADPH, which is the rate-limiting first step of the oxidative phase of the PPP. Compared to that in the wild type, the transcript level of G6PD1 in *gsm2* was reduced upon treatment with 1% Glc (Fig. 6b), indicating that the disruption of the $NADP^+$/NADPH balance may cause the inadequate production of protective antioxidants, such as glutathione (GSH) and thioredoxin ($Trx(SH)_2$). Second, in contrast to animals, in plants, E4P and PEP enter the shikimate pathway for the synthesis of three AAAs: phenylalanine (Phe), tyrosine (Tyr), and tryptophan (Trp). Of the metabolites derived from the three AAAs, Phe-derived plant secondary metabolites such as phenylpropanoids, flavonoids and anthocyanins are able to scavenge ROS and protect plants from stresses (Emiliani et al. 2013; Para et al. 2016; Xu and Rothstein 2018). The presumed depletion of E4P caused by GSM2 defect leads to the interruption of Phe synthesis and subsequently diverting Phe to a secondary metabolic pathway. Para et al. (2016) suggested that the supply of Phe could counteract ROS in young seedlings (Para et al. 2016). As expected, the Glc-induced chlorosis in *gsm2* cotyledons was recovered by the application of Phe but not Ery (Fig. 6c). On the other hand, RGS1, as a regulator of G-protein signaling, participates in Glc-induced autophagy (Janse van Rensburg, et al. 2019). Autophagy is a conserved process in the eukaryotic cell, which functions in the degradation or recycle of damaged proteins and organelles (Avin-Wittenberg 2019). Autophagy is thought of as a noncanonical antioxidant system to scavenge ROS for plant abiotic/biotic stress tolerance (Signorelli, et al. 2019). However, excess ROS in *gsm2* may inhibit Glc-induced autophagy by RGS1. Overall, the presence of a functional PPP is responsible for resistance to Glc-induced ROS stress.

GSM2 functions in cotyledon chloroplasts

GSM2 was localized to the chloroplasts (Fig. 3d), and chloroplasts act as metabolic centers not only for photosynthesis but for the biosynthesis of metabolites such as amino acids, nucleotides, and phytohormones (Rolland et al. 2012). Considering the endosymbiotic origin of chloroplasts, they have their own genome that coordinates with the nuclear genome to encode the chloroplast proteome (Daniell et al. 2016; Wu and Yan 2018). On sugar-free 1/2 MS medium, chloroplasts in cotyledons of both *gsm2* and the wild type showed well-formed thylakoid membrane systems (Fig. 3c). However, under high Glc condition, the misshapen chloroplasts were observed in *gsm2* cotyledons (Fig. 3c) and the damage of chloroplasts caused by the Glc-induced ROS was thought to occur at the early stage of chloroplast development (Supplementary Fig. S6). The development of chloroplasts is depended on light (Pogson and Albrecht 2011). In the dark, with or without treatment of Glc, *gsm2* and the wild type have no obvious difference with Trypan blue staining, showing almost etiolated cotyledons (Supplementary Fig. S9 left panel). Once plants were exposed to light, cell death was only detected in *gsm2* cotyledons treated with Glc (Supplementary Fig. S9 right panel), because functional chloroplasts has a complex redox regulatory network to combat ROS (Dietz et al. 2016). Chloroplast development in cotyledons and true leaves uses distinct pathways (Jarvis and Lopez-Juez 2013; Shimada et al. 2007). In cotyledons, etioplasts rapidly develop into chloroplasts under light conditions. In contrast, proplastids transform into chloroplasts during true leaf development. This may explain why cotyledons and not true leaves in *gsm2* exhibited chlorosis in response to Glc. Cotyledon development goes through hypogaeic to epigaeic growth, which belongs to early seedling growth of plants. Pogson et al. (2011) referred that even if chloroplast development is only impaired in cotyledons with normal chloroplast development in true leaves, plant growth and yield can be negatively impacted (Pogson and Albrecht 2011). As we observed before, besides the phenotype of chlorotic cotyledons, the growth of *gsm2* seedlings was inhibited upon treatment with Glc, suggesting the important role of GSM2 in early seedling growth. It has been established that both anterograde signaling and retrograde signaling between the chloroplasts and the nucleus serve to regulate chloroplast development, plant pathogen defense and the response to abiotic stresses (Kmiecik et al. 2016). A number of transcription factors participate in these signaling pathways (Van Aken et al. 2013). Recently, Dong et al. (2019) reported that the transcription factors TCP4 and PIF3 orchestrate to regulate cotyledon-specific light activation of *SAUR16* and *SAUR50* during de-etiolation in *Arabidopsis* (Dong et al. 2019). Further experiments needs to explain why cotyledons but not true leaves in *gsm2* exhibit chlorosis in response to Glc and how GSM2 functions in early seedling growth, especially for chloroplast development during hypogaeic and epigaeic seedling growth.

The Glc-induced chlorotic cotyledons of *gsm2* is not ABA dependent

It has been reported that Glc, as a signaling molecule, interacts with phytohormones to regulate plant growth and development (Sakr et al. 2018; Sheen 2014). ABA and ET are known to have antagonistic effects on the plant response to Glc (León 2003). Glc can induce ABA biosynthesis to establish a Glc-ABA signaling cascade and various ABA biosynthetic genes and signaling-related components participate in the cascade (Carvalho et al. 2016; Dekkers et al. 2008; Li et al. 2006; Rodrigues et al. 2013). Whereas, ET has an antagonizing effect on Glc signaling; for example, *eto1* and *ctr1* (ethylene overproducing and constitutive ethylene signaling mutants, respectively) displayed decreased glucose sensitivity (León 2003; Sakr et al. 2018). Numerous studies have provided evidence of the relationship between ROS and ABA or ET (Overmyer et al. 2003; Qi et al. 2017; Singh et al. 2017; Suzuki and Katano 2018). ROS are considered second messengers to participate in ABA-induced stomatal closure (Mittler and Blumwald 2015). Yang et al. (2014) have shown that the enhanced accumulation of ROS in *abo8*/*abo6*/*abo5* (aba-overly sensitive 8/6/5) leads to increased ABA sensitivity in these mutants during seed germination/root growth (He et al. 2012; Liu et al. 2010; Yang et al. 2014). While, ET and ROS also involves a complicated network in seed germination, cell death regulation and the plant immune response (Corbineau et al. 2014; Leymarie et al. 2012; Overmyer et al. 2003; Zipfel 2013). Recent research by Watkins et al. (2017) revealed that ethylene induces the accumulation of flavonol, which counteracts ROS and consequently inhibits ABA-induced stomatal closure in tomato (Watkins et al. 2017). *gsm2* still displayed chlorotic cotyledons in the absence of endogenous ABA in response to Glc (Supplementary Fig. S13a), suggesting that the Glc-induced chlorosis in *gsm2* cotyledons is ABA-independent. But ACC treatment may be able to alleviate Glc-induced chlorosis in *gsm2* cotyledons (Supplementary Fig. S13b). Interestingly, ET plays a regulatory role in photosynthesis depending on plant species and age, and it generally induces the degradation of chlorophyll to promote chlorosis in mature leaves (Ceusters and Van de Poel 2018). Therefore, how ET functions in the Glc-induced chlorosis in *gsm2* cotyledons needs further study.

In conclusion, this study extends our understanding of the role of the plant PPP in the maintenance of redox balance under normal or stress conditions. From a mutant screen based on Glc sensitivity, we isolated a Glc-hypersensitive mutant, *gsm2*, with a chlorotic-cotyledon

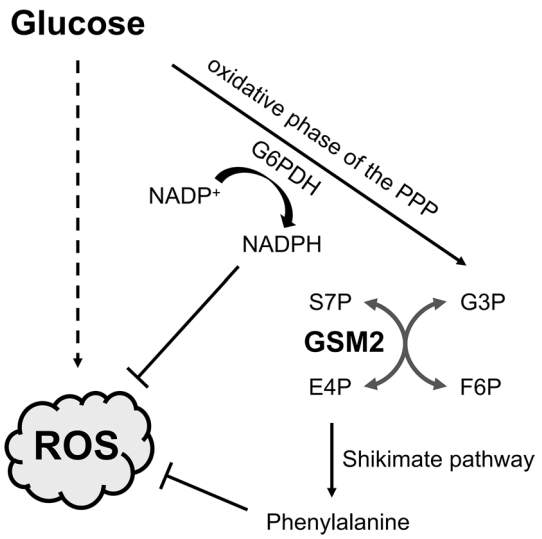

Fig. 7 Model of GSM2 regulation of the maintenance of ROS homeostasis in response to Glc during early seedling growth. As an alternative to glycolysis, Glc can go through the PPP. As a substrate of G6PDH, G6P is oxidized to yield 6-phosphogluconate (6PG), and, in the process, $NADP^+$ is converted to NADPH, which is able to participate in the reduction of glutathione and thioredoxin to defend against oxidative damage in the oxidative phase of the PPP. GSM2 functions in the non-oxidative phase of the PPP for the generation of E4P, which is used for the synthesis of AAAs and secondary metabolites via the shikimate pathway. Some of these compounds (such as Phe and flavonoids) have been reported to combat ROS

phenotype. *GSM2* encodes a transaldolase that is localized to the chloroplasts, and analysis of *gsm2* mutants indicates that GSM2 is involved in ABA-independent ROS homeostasis. We therefore propose a model for the response to Glc in which GSM2 functions in the PPP, leading to increased NADPH production and favoring carbon flux toward the shikimate pathway for antioxidant generation to combat oxidative stress (Fig. 7). GSM2 provides an interesting link between Glc, the PPP and ROS homeostasis in plants, and more details of this molecular network remain to be determined in the near future.

Acknowledgements This work was supported by the National Natural Science Foundation of China (31600987) and the Program for Innovation Team Building at Institution of Higher Education in Chongqing (CXTDX201601009).

Author contributions Y-FH and MZ designed the research. MZ, CZ, TY and JQ performed the experiments. MZ, CZ and Y-FH analyzed the data. MZ and Y-FH wrote the manuscript. All authors read and approved the manuscript. MZ and CZ contributed equally to this work.

Compliance with ethical standards

Conflict of interest The authors have no conflicts of interest to declare.

References

Avin-Wittenberg T (2019) Autophagy and its role in plant abiotic stress management. Plant Cell Environ 42:1045–1053

Bennett CF, Kwon JJ, Chen C, Russell J, Acosta K, Burnaevskiy N, Crane MM, Bitto A, Vander Wende H, Simko M, Pineda V, Rossner R, Wasko BM, Choi H, Chen S, Park S, Jafari G, Sands B, Perez Olsen C, Mendenhall AR, Morgan PG, Kaeberlein M (2017) Transaldolase inhibition impairs mitochondrial respiration and induces a starvation-like longevity response in *Caenorhabditis elegans*. PLoS Genet 13:e1006695

Caillau M, Paul Quick W (2005) New insights into plant transaldolase. Plant J 43:1–16

Carvalho RF, Szakonyi D, Simpson CG, Barbosa IC, Brown JW, Baena-Gonzalez E, Duque P (2016) The Arabidopsis SR45 splicing factor, a negative regulator of sugar signaling, modulates SNF1-related protein kinase 1 stability. Plant Cell 28:1910–1925

Ceusters J, Van de Poel B (2018) Ethylene exerts species-specific and age-dependent control of photosynthesis. Plant Physiol 176:2601–2612

Clough SJ, Bent AF (1998) Floral dip: a simplified method for Agrobacterium-mediated transformation of *Arabidopsis thaliana*. Plant J 16:735–743

Corbineau F, Xia Q, Bailly C, El-Maarouf-Bouteau H (2014) Ethylene, a key factor in the regulation of seed dormancy. Front Plant Sci 5:539

Couee I, Sulmon C, Gouesbet G, El Amrani A (2006) Involvement of soluble sugars in reactive oxygen species balance and responses to oxidative stress in plants. J Exp Bot 57:449–459

Czarnocka W, Karpinski S (2018) Friend or foe? Reactive oxygen species production, scavenging and signaling in plant response to environmental stresses. Free Radic Biol Med 122:4–20

Czechowski T, Stitt M, Altmann T, Udvardi MK, Scheible WR (2005) Genome-wide identification and testing of superior reference genes for transcript normalization in Arabidopsis. Plant Physiol 139:5–17

Daniell H, Lin CS, Yu M, Chang WJ (2016) Chloroplast genomes: diversity, evolution, and applications in genetic engineering. Genome Biol 17:134

Das K, Roychoudhury A (2014) Reactive oxygen species (ROS) and response of antioxidants as ROS-scavengers during environmental stress in plants. Front Environ Sci. https://doi.org/10.3389/fenvs.2014.00053s

de Vries L, Vanholme R, Van Acker R, De Meester B, Sundin L, Boerjan W (2018) Stacking of a low-lignin trait with an increased guaiacyl and 5-hydroxyguaiacyl unit trait leads to additive and synergistic effects on saccharification efficiency in *Arabidopsis thaliana*. Biotechnol Biofuels 11:257

Dekkers BJ, Schuurmans JA, Smeekens SC (2008) Interaction between sugar and abscisic acid signalling during early seedling development in Arabidopsis. Plant Mol Biol 67:151–167

Demidchik V (2015) Mechanisms of oxidative stress in plants: from classical chemistry to cell biology. Environ Exp Bot 109:212–228

Dietz KJ, Turkan I, Krieger-Liszkay A (2016) Redox- and reactive oxygen species-dependent signaling into and out of the photosynthesizing chloroplast. Plant Physiol 171:1541–1550

Dong T, Park Y, Hwang I (2015) Abscisic acid: biosynthesis, inactivation, homoeostasis and signalling. Essays Biochem 58:29–48

Dong J, Sun N, Yang J, Deng Z, Lan J, Qin G, He H, Deng XW, Irish VF, Chen H, Wei N (2019) The transcription factors TCP4 and PIF3 antagonistically regulate organ-specific light induction of SAUR genes to modulate cotyledon opening during de-etiolation in arabidopsis. Plant Cell 5:1155–1170

Emiliani J, Grotewold E, Falcone Ferreyra ML, Casati P (2013) Flavonols protect Arabidopsis plants against UV-B deleterious effects. Mol Plant 6:1376–1379

Foyer CH, Noctor G (2005) Redox homeostasis and antioxidant signaling: a metabolic interface between stress perception and physiological responses. Plant Cell 17:1866–1875

Fu Y, Lim S, Urano D, Tunc-Ozdemir M, Phan NG, Elston TC, Jones AM (2014) Reciprocal encoding of signal intensity and duration in a glucose-sensing circuit. Cell 156:1084–1095

He J, Duan Y, Hua D, Fan G, Wang L, Liu Y, Chen Z, Han L, Qu LJ, Gong Z (2012) DEXH box RNA helicase-mediated mitochondrial reactive oxygen species production in Arabidopsis mediates crosstalk between abscisic acid and auxin signaling. Plant Cell 24:1815–1833

Holscher C, Meyer T, von Schaewen A (2014) Dual-targeting of Arabidopsis 6-phosphogluconolactonase 3 (PGL3) to chloroplasts and peroxisomes involves interaction with Trx m2 in the cytosol. Mol Plant 7:252–255

Hsiao YC, Hsu YF, Chen YC, Chang YL, Wang CS (2016) A WD40 protein, AtGHS40, negatively modulates abscisic acid degrading and signaling genes during seedling growth under high glucose conditions. J Plant Res 129:1127–1140

Hsu YF, Chen YC, Hsiao YC, Wang BJ, Lin SY, Cheng WH, Jauh GY, Harada JJ, Wang CS (2014) AtRH57, a DEAD-box RNA helicase, is involved in feedback inhibition of glucose-mediated abscisic acid accumulation during seedling development and additively affects pre-ribosomal RNA processing with high glucose. Plant J 77:119–135

Huang L, Yu LJ, Zhang X, Fan B, Wang FZ, Dai YS, Qi H, Zhou Y, Xie LJ, Xiao S (2019) Autophagy regulates glucose-mediated root meristem activity by modulating ROS production in Arabidopsis. Autophagy 15:407–422

Janse van Rensburg HC, Van den Ende W (2017) UDP-glucose: a potential signaling molecule in plants? Front Plant Sci 8:2230

Janse van Rensburg HC, Van den Ende W, Signorelli S (2019) Autophagy in plants: both a puppet and a puppet master of sugars. Front Plant Sci 10:14

Jarvis P, Lopez-Juez E (2013) Biogenesis and homeostasis of chloroplasts and other plastids. Nat Rev Mol Cell Biol 14:787–802

Keunen E, Peshev D, Vangronsveld J, Van Den Ende W, Cuypers A (2013) Plant sugars are crucial players in the oxidative challenge during abiotic stress: extending the traditional concept. Plant Cell Environ 36:1242–1255

Kleniewska P, Piechota A, Skibska B, Goraca A (2012) The NADPH oxidase family and its inhibitors. Arch Immunol Ther Exp (Warsz) 60:277–294

Kmiecik P, Leonardelli M, Teige M (2016) Novel connections in plant organellar signalling link different stress responses and signalling pathways. J Exp Bot 67:3793–3807

Kruger NJ, von Schaewen A (2003) The oxidative pentose phosphate pathway: structure and organisation. Curr Opin Plant Biol 6:236–246

Kumari P, Reddy CR, Jha B (2015) Methyl Jasmonate-induced lipidomic and biochemical alterations in the intertidal macroalga *Gracilaria dura* (Gracilariaceae, Rhodophyta). Plant Cell Physiol 56:1877–1889

León P (2003) Sugar and hormone connections. Trends Plant Sci 8:110–116

Leymarie J, Vitkauskaite G, Hoang HH, Gendreau E, Chazoule V, Meimoun P, Corbineau F, El-Maarouf-Bouteau H, Bailly C (2012) Role of reactive oxygen species in the regulation of Arabidopsis seed dormancy. Plant Cell Physiol 53:96–106

Li L, Sheen J (2016) Dynamic and diverse sugar signaling. Curr Opin Plant Biol 33:116–125

Li Y, Lee KK, Walsh S, Smith C, Hadingham S, Sorefan K, Cawley G, Bevan MW (2006) Establishing glucose- and ABA-regulated transcription networks in Arabidopsis by microarray analysis and promoter classification using a relevance vector machine. Genome Res 16:414–427

Liu Y, He J, Chen Z, Ren X, Hong X, Gong Z (2010) ABA overly-sensitive 5 (ABO5), encoding a pentatricopeptide repeat protein required for cis-splicing of mitochondrial nad2 intron 3, is involved in the abscisic acid response in Arabidopsis. Plant J 63:749–765

Luo J, Xiang Y, Xu X, Fang D, Li D, Ni F, Zhu X, Chen B, Zhou M (2018) High glucose-induced ROS production stimulates proliferation of pancreatic cancer via inactivating the JNK pathway. Oxid Med Cell Longev 2018:6917206

Maeda H, Dudareva N (2012) The shikimate pathway and aromatic amino acid biosynthesis in plants. Annu Rev Plant Biol 63:73–105

Maloney GS, DiNapoli KT, Muday GK (2014) The anthocyanin reduced tomato mutant demonstrates the role of flavonols in tomato lateral root and root hair development. Plant Physiol 166:614–631

Mhamdi A, Van Breusegem F (2018) Reactive oxygen species in plant development. Development 145:dev164376

Mira M, Hill RD, Stasolla C (2016) Regulation of programmed cell death by phytoglobins. J Exp Bot 67:5901–5908

Mittler R (2017) ROS are good. Trends Plant Sci 22:11–19

Mittler R, Blumwald E (2015) The roles of ROS and ABA in systemic acquired acclimation. Plant Cell 27:64–70

Moehs CP, Allen PV, Friedman M, Belknap WR (1996) Cloning and expression of transaldolase from potato. Plant Mol Biol 32:447–452

Moore B, Zhou L, Rolland F, Hall Q, Cheng WH, Liu YX, Hwang I, Jones T, Sheen J (2003) Role of the Arabidopsis glucose sensor HXK1 in nutrient, light, and hormonal signaling. Science 300:332–336

Muhlemann JK, Younts TLB, Muday GK (2018) Flavonols control pollen tube growth and integrity by regulating ROS homeostasis during high-temperature stress. Proc Natl Acad Sci USA 115:E11188–E11197

Overmyer K, Brosché M, Kangasjärvi J (2003) Reactive oxygen species and hormonal control of cell death. Trends Plant Sci 8:335–342

Para A, Muhammad D, Orozco-Nunnelly DA, Memishi R, Alvarez S, Naldrett MJ, Warpeha KM (2016) The dehydratase ADT3 Affects ROS homeostasis and cotyledon development. Plant Physiol 172:1045–1060

Parthasarathy A, Cross PJ, Dobson RCJ, Adams LE, Savka MA, Hudson AO (2018) A three-ring circus: metabolism of the three proteogenic aromatic amino acids and their role in the health of plants and animals. Front Mol Biosci 5:29

Perl A, Qian Y, Chohan KR, Shirley CR, Amidon W, Banerjee S, Middleton FA, Conkrite KL, Barcza M, Gonchoroff N, Suarez SS, Banki K (2006) Transaldolase is essential for maintenance of the mitochondrial transmembrane potential and fertility of spermatozoa. Proc Natl Acad Sci USA 103:14813–14818

Perl A, Hanczko R, Telarico T, Oaks Z, Landas S (2011) Oxidative stress, inflammation and carcinogenesis are controlled through the pentose phosphate pathway by transaldolase. Trends Mol Med 17:395–403

Pogson BJ, Albrecht V (2011) Genetic dissection of chloroplast biogenesis and development: an overview. Plant Physiol 155:1545–1551

Porra RJ (2002) The chequered history of the development and use of simultaneous equations for the accurate determination of chlorophylls a and b. Photosynth Res 73:149–156

Qi J, Wang J, Gong Z, Zhou JM (2017) Apoplastic ROS signaling in plant immunity. Curr Opin Plant Biol 38:92–100

Qian Y, Banerjee S, Grossman CE, Amidon W, Nagy G, Barcza M, Niland B, Karp DR, Middleton FA, Banki K, Perl A (2008) Transaldolase deficiency influences the pentose phosphate

pathway, mitochondrial homoeostasis and apoptosis signal processing. Biochem J 415:123–134
Raja V, Majeed U, Kang H, Andrabi KI, John R (2017) Abiotic stress: interplay between ROS, hormones and MAPKs. Environ Exp Bot 137:142–157
Rodrigues A, Adamo M, Crozet P, Margalha L, Confraria A, Martinho C, Elias A, Rabissi A, Lumbreras V, Gonzalez-Guzman M, Antoni R, Rodriguez PL, Baena-Gonzalez E (2013) ABI1 and PP2CA phosphatases are negative regulators of Snf1-related protein kinase1 signaling in Arabidopsis. Plant Cell 25:3871–3884
Rolland N, Curien G, Finazzi G, Kuntz M, Marechal E, Matringe M, Ravanel S, Seigneurin-Berny D (2012) The biosynthetic capacities of the plastids and integration between cytoplasmic and chloroplast processes. Annu Rev Genet 46:233–264
Sakr S, Wang M, Dedaldechamp F, Perez-Garcia MD, Oge L, Hamama L, Atanassova R (2018) The sugar-signaling hub: overview of regulators and interaction with the hormonal and metabolic network. Int J Mol Sci 19:2506
Schulz TJ, Zarse K, Voigt A, Urban N, Birringer M, Ristow M (2007) Glucose restriction extends *Caenorhabditis elegans* life span by inducing mitochondrial respiration and increasing oxidative stress. Cell Metab 6:280–293
Semenza GL (2017) Hypoxia-inducible factors: coupling glucose metabolism and redox regulation with induction of the breast cancer stem cell phenotype. EMBO J 36:252–259
Shah MS, Brownlee M (2016) Molecular and cellular mechanisms of cardiovascular disorders in diabetes. Circ Res 118:1808–1829
Sheen J (2014) Master regulators in plant glucose signaling networks. J Plant Biol 57:67–79
Shigeoka S, Maruta T (2014) Cellular redox regulation, signaling, and stress response in plants. Biosci Biotechnol Biochem 78:1457–1470
Shimada H, Mochizuki M, Ogura K, Froehlich JE, Osteryoung KW, Shirano Y, Shibata D, Masuda S, Mori K, Takamiya K (2007) Arabidopsis cotyledon-specific chloroplast biogenesis factor CYO1 is a protein disulfide isomerase. Plant Cell 19:3157–3169
Signorelli S, Tarkowski LP, Van den Ende W, Bassham DC (2019) Linking autophagy to abiotic and biotic stress responses. Trends Plant Sci 24:413–430
Singh R, Parihar P, Singh S, Mishra RK, Singh VP, Prasad SM (2017) Reactive oxygen species signaling and stomatal movement: current updates and future perspectives. Redox Biol 11:213–218
Stincone A, Prigione A, Cramer T, Wamelink MM, Campbell K, Cheung E, Olin-Sandoval V, Gruning NM, Kruger A, Tauqeer Alam M, Keller MA, Breitenbach M, Brindle KM, Rabinowitz JD, Ralser M (2015) The return of metabolism: biochemistry and physiology of the pentose phosphate pathway. Biol Rev Camb Philos Soc 90:927–963
Suzuki N, Katano K (2018) Coordination between ROS regulatory systems and other pathways under heat stress and pathogen attack. Front Plant Sci 9:490
Tanaka T, Tanaka H, Machida C, Watanabe M, Machida Y (2004) A new method for rapid visualization of defects in leaf cuticle reveals five intrinsic patterns of surface defects in Arabidopsis. Plant J 37:139–146
Tsukagoshi H (2016) Control of root growth and development by reactive oxygen species. Curr Opin Plant Biol 29:57–63
Van Aken O, Zhang B, Law S, Narsai R, Whelan J (2013) AtWRKY40 and AtWRKY63 modulate the expression of stress-responsive nuclear genes encoding mitochondrial and chloroplast proteins. Plant Physiol 162:254–271
Vanholme R, Storme V, Vanholme B, Sundin L, Christensen JH, Goeminne G, Halpin C, Rohde A, Morreel K, Boerjan W (2012) A systems biology view of responses to lignin biosynthesis perturbations in Arabidopsis. Plant Cell 24:3506–3529
Wang S, Moustaid-Moussa N, Chen L, Mo H, Shastri A, Su R, Bapat P, Kwun I, Shen CL (2014) Novel insights of dietary polyphenols and obesity. J Nutr Biochem 25:1–18
Waszczak C, Carmody M, Kangasjarvi J (2018) Reactive oxygen species in plant signaling. Annu Rev Plant Biol 69:209–236
Watkins JM, Chapman JM, Muday GK (2017) Abscisic acid-induced reactive oxygen species are modulated by flavonols to control stomata aperture. Plant Physiol 175:1807–1825
Wu W, Yan Y (2018) Chloroplast proteome analysis of *Nicotiana tabacum* overexpressing TERF1 under drought stress condition. Bot Stud 59:26
Xiao G, Zhou J, Lu X, Huang R, Zhang H (2018) Excessive UDPG resulting from the mutation of UAP1 causes programmed cell death by triggering reactive oxygen species accumulation and caspase-like activity in rice. New Phytol 217:332–343
Xu Z, Rothstein SJ (2018) ROS-Induced anthocyanin production provides feedback protection by scavenging ROS and maintaining photosynthetic capacity in Arabidopsis. Plant Signal Behav 13:e1451708
Yang L, Zhang J, He J, Qin Y, Hua D, Duan Y, Chen Z, Gong Z (2014) ABA-mediated ROS in mitochondria regulate root meristem activity by controlling PLETHORA expression in Arabidopsis. PLoS Genet 10:e1004791
Yang Z, Zhou Y, Huang J, Hu Y, Zhang E, Xie Z, Ma S, Gao Y, Song S, Xu C, Liang G (2015) Ancient horizontal transfer of transaldolase-like protein gene and its role in plant vascular development. New Phytol 206:807–816
Yoo SD, Cho YH, Sheen J (2007) Arabidopsis mesophyll protoplasts: a versatile cell system for transient gene expression analysis. Nat Protoc 2:1565–1572
Zheng M, Yang T, Tao P, Zhu C, Fu Y, Hsu YF (2019) Arabidopsis GSM1 is involved in ABI4-regulated ABA signaling under high-glucose condition in early seedling growth. Plant Sci 287:110183
Zipfel C (2013) Combined roles of ethylene and endogenous peptides in regulating plant immunity and growth. Proc Natl Acad Sci USA 110:5748–5749